

Comparison of Simultaneous PIV and Hydroxyl Tagging Velocimetry in Low Velocity Flows

Matthieu A. André¹, Philippe M. Bardet^{1,*}, Ross A. Burns², Paul M. Danehy³

1: Dept. of Mechanical Engineering, The George Washington University, Washington, DC, USA

2: National Institute of Aerospace, Hampton, VA, USA

3: NASA Langley Research Center, Hampton, VA, USA

* Correspondent author: bardet@gwu.edu

Keywords: MTV, Low speed flow, PIV comparison

ABSTRACT

Hydroxyl tagging velocimetry (HTV) is a molecular tagging velocimetry (MTV) technique that relies on the photo-dissociation of water vapor into OH radicals and their subsequent tracking using laser-induced fluorescence. At ambient temperature in air, the OH species lifetime is about 50 μ s. The feasibility of using HTV for probing low-speed flows (a few m/s) is investigated by using an inert, heated gas as a means to increase the OH species lifetime. Unlike particle-based techniques, MTV does not suffer from tracer settling, which is particularly problematic at low speeds. Furthermore, the flow needs to be seeded with only a small mole fraction of water vapor, making it safer for both the user and facilities than other MTV techniques based on corrosive or toxic chemical tracers.

HTV is demonstrated on a steam-seeded nitrogen jet at approximately 75 °C in the laminar ($U_{mean}=3.31$ m/s, $Re=1,540$), transitional ($U_{mean}=4.48$ m/s, $Re=2,039$), and turbulent ($U_{mean}=6.91$ m/s, $Re=3,016$) regimes at atmospheric pressure. The measured velocity profiles are compared with particle image velocimetry (PIV) measurements performed simultaneously with a second imager. Seeding for the PIV is achieved by introducing micron-sized water droplets into the flow with the steam; the same laser sheet is used for PIV and HTV to guarantee spatial and temporal overlap of the data. Optimizing each of these methods, however, requires conflicting operating conditions: higher temperatures benefit the HTV signals but reduce the available seed density for the PIV through evaporation. Nevertheless, data are found to agree within 10% for the instantaneous velocity profiles and within 5% for the mean profiles and demonstrate the feasibility of HTV for low-speed flows at moderate to high temperatures.

1. Introduction

Molecular tagging velocimetry (MTV) [Tropea, 2007] is an alternative measurement technique to the well-established, non-intrusive flow diagnostic that is particle image velocimetry (PIV) [Adrian, 2005]. Both MTV and PIV are time-of-flight measurement techniques used to obtain velocity; however, rather than using discrete particles like PIV, the tracers used in MTV are molecular or atomic species. MTV has been applied in both gaseous and liquid flows [Tropea, 2007]. It is therefore important to understand the precision and accuracy of this technique. While

such an understanding is achievable through direct comparison to PIV, a simultaneous measurement has not been reported to date. Herein, PIV and MTV are acquired simultaneously in a gas-phase jet to provide a direct comparison between the two methods. In these preliminary studies, both laminar and turbulent jets have been tested with a focus on characterizing uncertainties in the MTV measurements for low-speed flows.

In a particle-free gas phase, several techniques exist to “tag,” or mark, a species of interest. The most common measurement scheme involves the creation or excitation of a radical chemical species and subsequently tracking its motion with planar laser-induced fluorescence (PLIF). Molecular tracers have the advantage of no settling or slip velocity, which allows them to accurately follow quiescent and hypersonic flows alike [Danehy, 2003]. Furthermore, these tracers can also be created in gas flows that are typically challenging to seed for PIV, such as high-temperature or reacting flows, and in environments where particles are undesirable.

As motivation for these studies, MTV is being adapted for resolving velocity in a simulator of a high-temperature gas-cooled nuclear reactor [André, 2015]. In this application, it is necessary to measure long-duration flow transients encountered in simulated accident conditions, where temperature and flow rates vary slowly (on the order of minutes to hours). In addition to these slow phenomena, for some events (such as flow reversal) the mean velocity can be very small (on the order of 1 m/s or less). Moreover, solid particles, which are negatively buoyant, will likely settle, resulting in loss of signal and also will contaminate the facility and negatively influence radiative heat transfer. For this application, MTV could prove to be a viable alternative to particle-based methods. Some of the drawbacks of MTV include lower spatial resolution due to diffusion of tracers, limited tracer lifetime, and a more complicated setup compared to PIV. Also MTV measurements are usually made at a point, along a line, or on a coarse grid of lines whereas PIV can be performed in planes or even volumes.

To date, low speed flows (~2 m/s) have been successfully probed using ozone tagging velocimetry (OTV); however, these tracers are not suited for high temperature flows due to reduced species lifetime and O₃ peak concentration [Pitz, 2000], and O₂ will oxidize structural materials in the facility. As an alternative to OTV, the present study instead utilizes hydroxyl tagging velocimetry (HTV). HTV makes use of hydroxyl radicals (OH) created from water vapor. The advantages of this tracer species include non-toxicity, ease of adding the tracer (water vapor) to the test gas, and relatively long tracer lifetime at high temperatures [Ribarov, 2002]. H₂O is also present at high temperature in most combustion products, which makes HTV a very convenient technique for probing such flows [Ribarov, 2004]. OH radicals are typically created with an argon-fluoride excimer laser (output at 193 nm) through a photo-dissociation process

whose efficiency is temperature-dependent. The dissociation fraction increases by an order of magnitude between ambient temperature and flame temperature [Ribarov, 2004]. OH offers several vibrational transitions in the ultraviolet (UV) portion of the spectrum, all from the $A^2\Sigma^+-X^2\Pi$ electronic transition, as shown in the spectrum of Fig. 1 obtained with LIFBASE [Luque, 1999], that can be excited with PLIF. It should be noted that when exciting the (0,0) band around 308 nm, the resulting fluorescence occurs in the same spectral region and prevents the use of a filter to remove scattered laser light. Therefore, although the fluorescent emission is stronger when exciting that band, the acquired images are more likely to be contaminated by scattered laser light from particles and nearby surfaces. Thus, the signal-to-noise ratio (SNR) was found to be higher for excitation of the (1,0) band combined with spectral filtering of the signal.

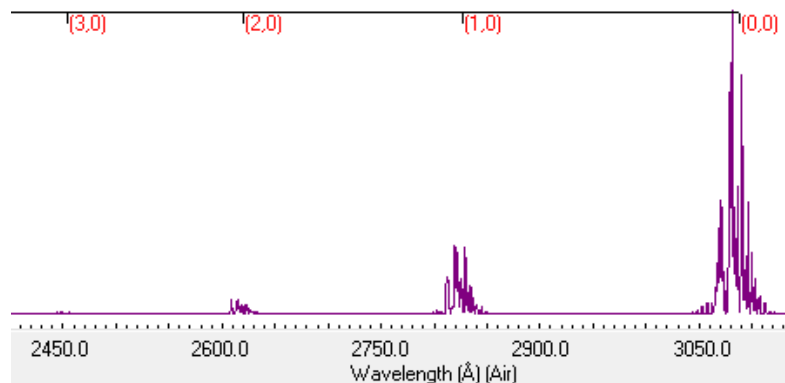


Fig. 1 LIFBASE computed fluorescence excitation spectrum of $A^2\Sigma^+-X^2\Pi$ electronic transition of OH in air at 300 K and 1 atm. The first four vibrational transitions all originating from the ground vibrational state are shown here

2. Experimentation and Test Procedure

a. HTV diagnostics

The HTV system is composed of an excimer laser (write pulse) and a dual-pulse, tunable dye laser (read pulses), which are mounted on a cart to allow for transportation to experimental facilities. A diagram of this laser system is shown in Fig. 2. The excimer laser (GAM EX5A) outputs a 10 mJ/pulse beam at 193 nm to photo-dissociate H₂O into OH. This beam is focused in the measurement region using a 300 mm focal length spherical lens, resulting in a 0.7 mm wide tag line. The output of two frequency-doubled Nd:YAG lasers (10 Hz, 0.5 J/pulse, 532 nm, Spectra Physics Quanta Ray Lab 170) are combined to pump a tunable dye laser (Sirah Cobra-Stretch). A 15 mm wide by 3 mm thick sheet, overlapping with the excimer beam, is formed in the measurement region using a 200 mm focal length cylindrical lens. The dual-pulse configuration, combined with double-framed imaging, allows the data to be corrected for potential wandering of

the write laser beam caused by beam pointing or vibration and hence leads to improved measurement precision in comparison to using only a single read pulse.

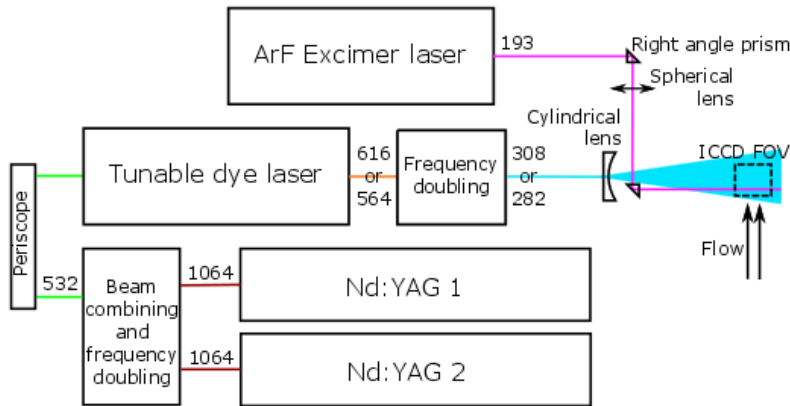


Fig. 2 Setup of the lasers used for “write” and “read” pulses. Wavelengths are given in nm.

The present work focuses on exciting the (1,0) vibrational transition of OH. Fine-tuning of the PLIF excitation wavelength maximizes the fluorescence signal. Use of the Q₁(1) absorption line in the (1,0) band at 281.905 nm allowed the use of long-pass filters (Schott WG 295 and WG 305) to filter out the Mie scattering from the PIV tracers and increase the SNR of the PLIF signal.

The fluorescence signal from the read pulses is recorded with a time-gated ICCD (PCO DiCam Pro, 6.7 micron square pixels) set at 75% of maximum gain. A UV-transmitting Nikon 105 mm f/4.5 lens is mounted on the image intensifier with a 15 mm extension tube and provided a resolution of 35.5 pixels/mm. The gate time of the intensifier is set at 1 μ s and temporally centered on the PLIF signal to minimize background noise. This gate duration was chosen because it was expected to be much longer than the OH fluorescence lifetime, estimated to be a few ns. So-called “background” images were acquired after HTV data was acquired by blocking the excimer laser pulses. These were subtracted from the raw data images in post-processing.

b. Simultaneous PIV diagnostics

PIV is performed simultaneously with the dye laser pulses using a second intensified camera to record Mie scattering from PIV tracers (micron-sized droplets) that are injected in the flow. A 50/50 UV beam splitter plate directs the Mie scattered light and fluorescence to both cameras, which are oriented normal to each other as shown in Fig. 3. The PIV camera is an image intensifier (LaVision IRO25) lens-coupled to a 12-bit CCD camera (QImaging QIClick). The intensifier is necessary to convert the UV signal from the Mie scattering to a wavelength the

camera can record because the CCD sensor does not respond below 300 nm. The gate time is set at 300 ns to minimize the collection of background light and is temporally centered on the dye laser pulses. An identical lens as was used with the HTV camera was used with a 25 mm extension ring, leading to a resolution of 40.8 pixels/mm. No spectral filtering is required because the scattered PIV signal is orders of magnitude stronger than the fluorescence signal, and requires a gain of only 44% of maximum to be properly imaged. All HTV and PIV instruments are synchronized using a pulse generator (Berkeley Nucleonics 575) with an accuracy of 250 ps and are monitored with a high-speed, digital oscilloscope (Agilent MSOX-3054A).

Note that at elevated temperatures, the PIV seeding is limited due to the evaporation of droplets. However, higher temperature conditions improve the quality of the HTV data because of the higher H₂O (vapor) content and superior OH production efficiency [Pitz, 2000].

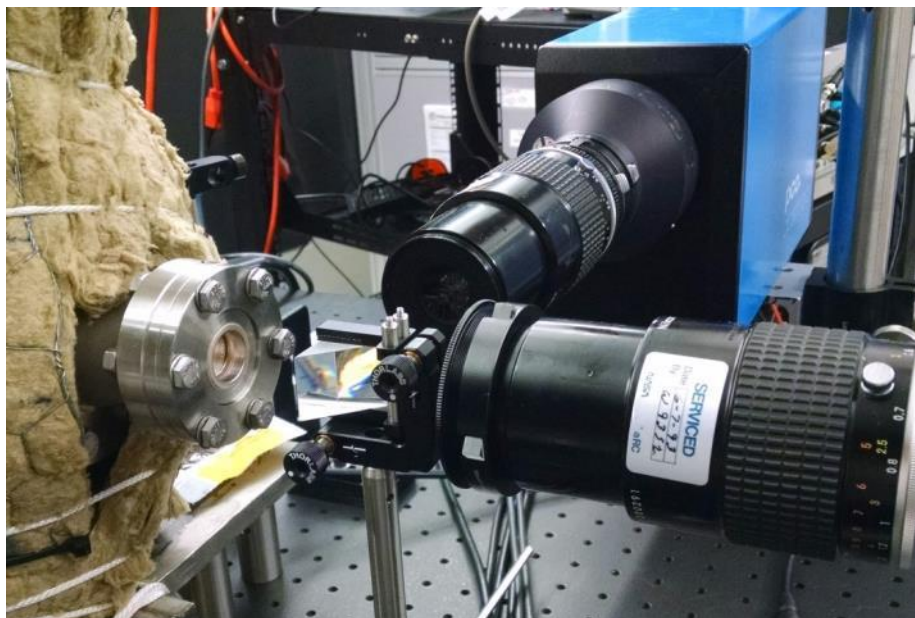


Fig. 3 PIV/HTV imaging setup. The prism shown here is replaced with a 50/50 UV beam-splitter plate when simultaneous PIV/HTV data are recorded

c. Test flow

The data are acquired at ambient pressure and with temperature in the range of 344 to 363 K. Compressed nitrogen is pressure-regulated, bubbled through water in a TSI 6-jet atomizer, and exits a 9.02 mm inner diameter vertical pipe with a straight entry length of 40 diameters. The atomizer enables both seeding of the jet with both PIV tracers (water droplets) and water vapor for the HTV excitation. The jet is enclosed in a chamber with two UV-grade sapphire viewports mounted perpendicularly to the jet axis (see Fig. 4). The lasers enter one window and the

cameras viewed the laser sheet from a perpendicular view via the other window. To increase the temperature of the flow, heating tape is wrapped around the body of the flow chamber and inlet tube and is controlled by a digital controller to adjust the test conditions. A thermocouple affixed near the tube exit measures the flow temperature. The flow rate is precisely controlled with a Brooks Instrument thermal mass flow controller (Accuracy: 0.5% of reading + 0.1% full scale). The mass flow rate is varied between 0.5 ± 0.03 and 1.8 ± 0.04 kg/h, which corresponds to a range of Reynolds number based on mean velocity and the tube inner diameter of 1,000-4,000. The chamber top is open to the atmosphere guaranteeing ambient pressure in the chamber.



Fig. 4 Test chamber containing the vertical jet. Laser port on the left and camera port on the right

3. Results

To demonstrate and validate the HTV technique over a range of test conditions, laminar and turbulent jet data are investigated. Table 1 summarizes the test flow conditions. U_{mean} is the jet mean velocity calculated using a mass flow-meter upstream of the nozzle. Mean and instantaneous stream-wise velocity profiles recorded 3 mm downstream of the nozzle are presented here.

| Q (kg/h) | P (atm) | T (K) | dt (μ s) | U_{mean} (m/s) | Re |
|------------|-----------|---------|-----------------|------------------|-------|
| 0.75 | 1 | 344 | 250 | 3.31 | 1,540 |
| 1 | 1 | 347 | 250 | 4.48 | 2,039 |
| 1.5 | 1 | 363 | 250 | 6.91 | 3,016 |

Table 1 Test matrix

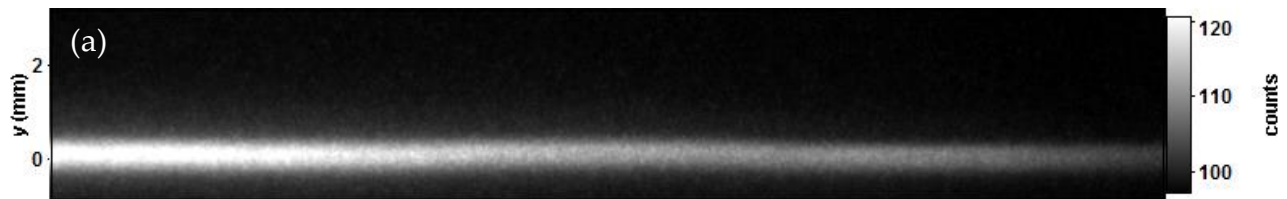
a. HTV data

HTV data are recorded with a time separation of 250 μs between read pulses in all cases. The first read pulse is emitted about 5 μs after the write pulse. Figure 5, top, shows one such mean PLIF image, where the tagged line is very close to a straight line due to the small delay between write and read pulse. Both laser beams enter the field of view on the left, and are visibly attenuated along their paths. The attenuation is mostly due to scattering from the water droplets used for PIV. Attenuation of the excimer beam by photo-dissociation (conversion of H₂O vapor to OH) is only a few percent over the field of view and thus comprises a small fraction of the observed decrease in signal. The line is relatively wide (~25 pixels, or 0.7 mm) by MTV standards but could be decreased by using a shorter focal distance lens for focusing the excimer beam. The three subsequent images of Fig. 5 show the mean PLIF image of the line 250 μs later for different Reynolds numbers. OH tracers have been advected by the flow in addition to molecular diffusion.

For $Re=1,540$, the jet is laminar and the profile appears nearly parabolic. At $Re=3,016$, the jet is turbulent and the profile has a flatter top associated with turbulent flow. $Re=2,039$ is in the transitional regime and exhibits a slight asymmetry that can be explained by the boundary layer transitioning to turbulent at different location around the pipe upstream of the nozzle.

Figure 5 (e) presents an instantaneous PLIF image for $Re=3,016$ which shows the low SNR of these images. 360 pairs of such instantaneous image are processed individually for each case. Velocity is obtained by measuring the line displacement between image pairs via curve-fitting the stream-wise intensity profile. Due to the noisy nature of the data, images are horizontally binned over 20 pixels. Outliers are then filtered based on the difference with the neighboring points. The velocity profile is then averaged. A second processing pass uses this averaged profile to refine the region to look for the HTV signal and to further eliminate outliers that arise from bright spots away from the line such as at the top right of Fig. 5 (e).

Instantaneous and averaged profiles are presented in the next section.



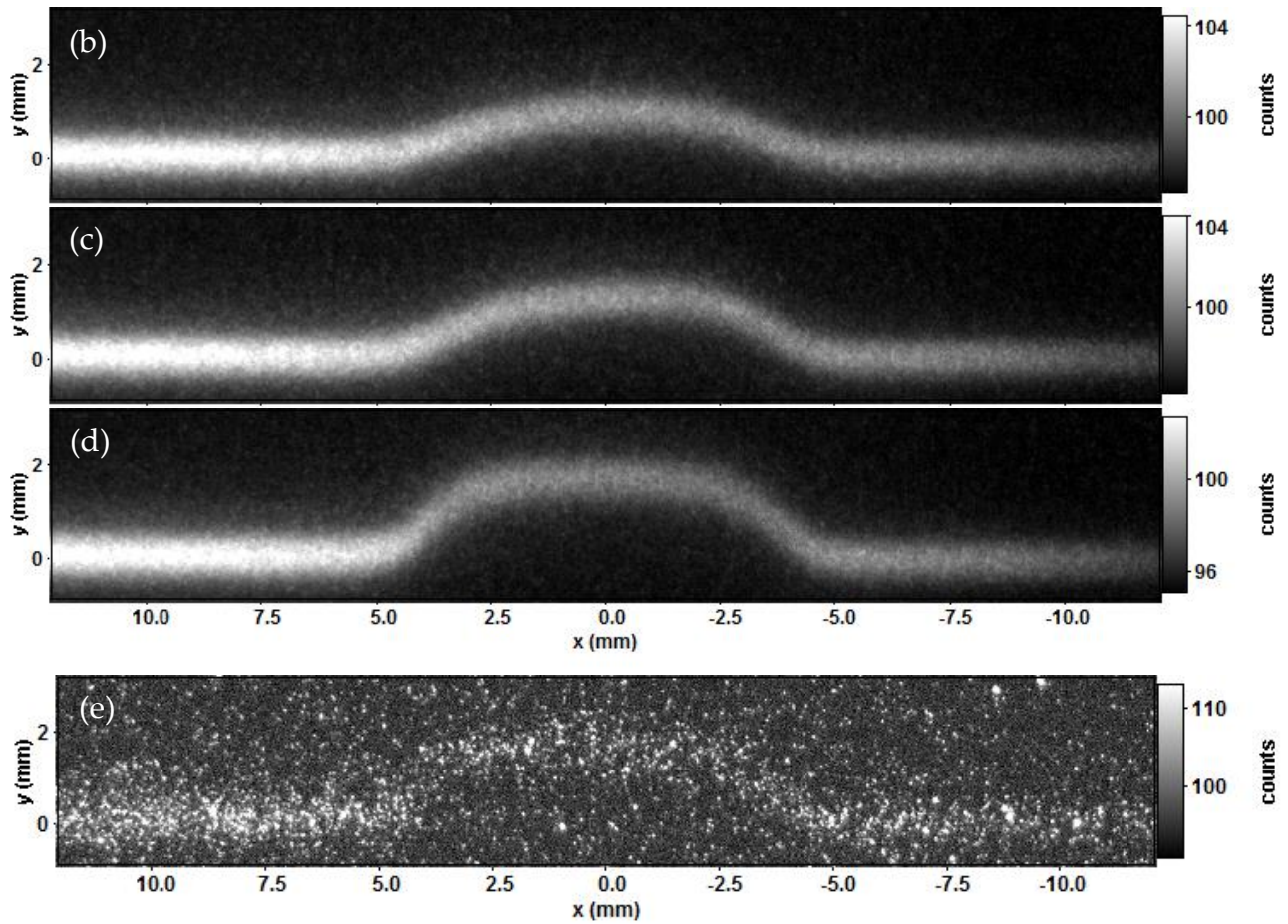


Fig. 5 PLIF images. Intensity is scaled to the min-max of each image. Mean PLIF line 5 μ s after write pulse for $Re=1,540$ (a), mean PLIF line 250 μ s after first read pulse for $Re=1,540$ (b), $Re=2,039$ (c), and $Re=3,016$ (d), single-shot image of PLIF line at $dt=250$ μ s for $Re=3,016$ (e).

b. PIV data

PIV data recorded at the same time as the HTV data are processed with LaVision Davis 8.3 software using a multi-pass cross-correlation scheme with constant size interrogation window (96 pixels with a 4:1 vertical elliptical weighting) with a 75% overlap, resulting in a vector spacing of 24 pixels. As for the HTV processing, a preliminary mean velocity field is computed and used as an initial guess for the cross correlation algorithm. To directly compare HTV with PIV, the PIV data are linearly interpolated at the location of the HTV datapoints. Stream-wise velocity profiles are extracted at the location corresponding to the HTV region. The RMS deviation from the mean is also computed for PIV.

c. PIV/HTV instantaneous profiles comparison

For each flow regime, 200 instantaneous velocity profiles are compared. The agreement is quantified using the RMS (root mean square) of the difference (or error) between the two techniques for the velocity along the profile: $\epsilon_{RMS} = \frac{1}{U_{mean}} \sqrt{\sum \frac{(u_{PIV} - u_{HTV})^2}{n_{points}}}$, where n_{points} is the number of datapoint per profile. Results are normalized by the respective mean velocity obtained from the flowmeter, and expressed in percent. The distribution of the RMS error for 200 samples is presented in the normalized histograms shown in Fig. 6.

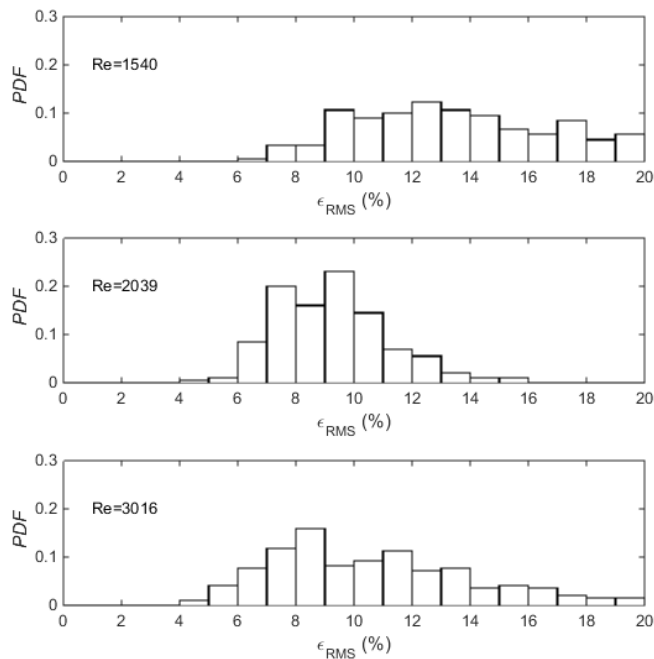


Fig. 6 Normalized histograms showing the distribution of RMS error between PIV and HTV for the three regimes

The median RMS error is 13.5%, 9.1%, and 10.3% for the $Re=1,540$, $Re=2,039$, and $Re=3,016$ conditions, and the lowest is 6.9%, 4.5%, and 4.1% in the same order. The higher observed error at $Re=1,540$ is caused by difficulties in properly seeding the flow with PIV tracers since the amount of droplets generated in the atomizer depends on pressure and flow rate. The lowest median error is obtained for the $Re=2,039$ case. At $Re=3,016$, the error increases as a result of the turbulent flow leading more diffuse tag lines in the HTV images.

Figure 7 shows comparisons of single-shot HTV/PIV velocity profiles for each case. The left column shows a ‘typical’ instantaneous profile for which the RMS error is equal to the median, while the right column shows the best instantaneous profile (lowest RMS error). As seen in Fig.

5, the single-shot HTV signal is relatively weak, which results in noisy instantaneous velocity profiles. Furthermore, the PIV data also suffer from low seeding density. Nevertheless, on most profiles, the general shape of the profile is still captured to some degree by both methods.

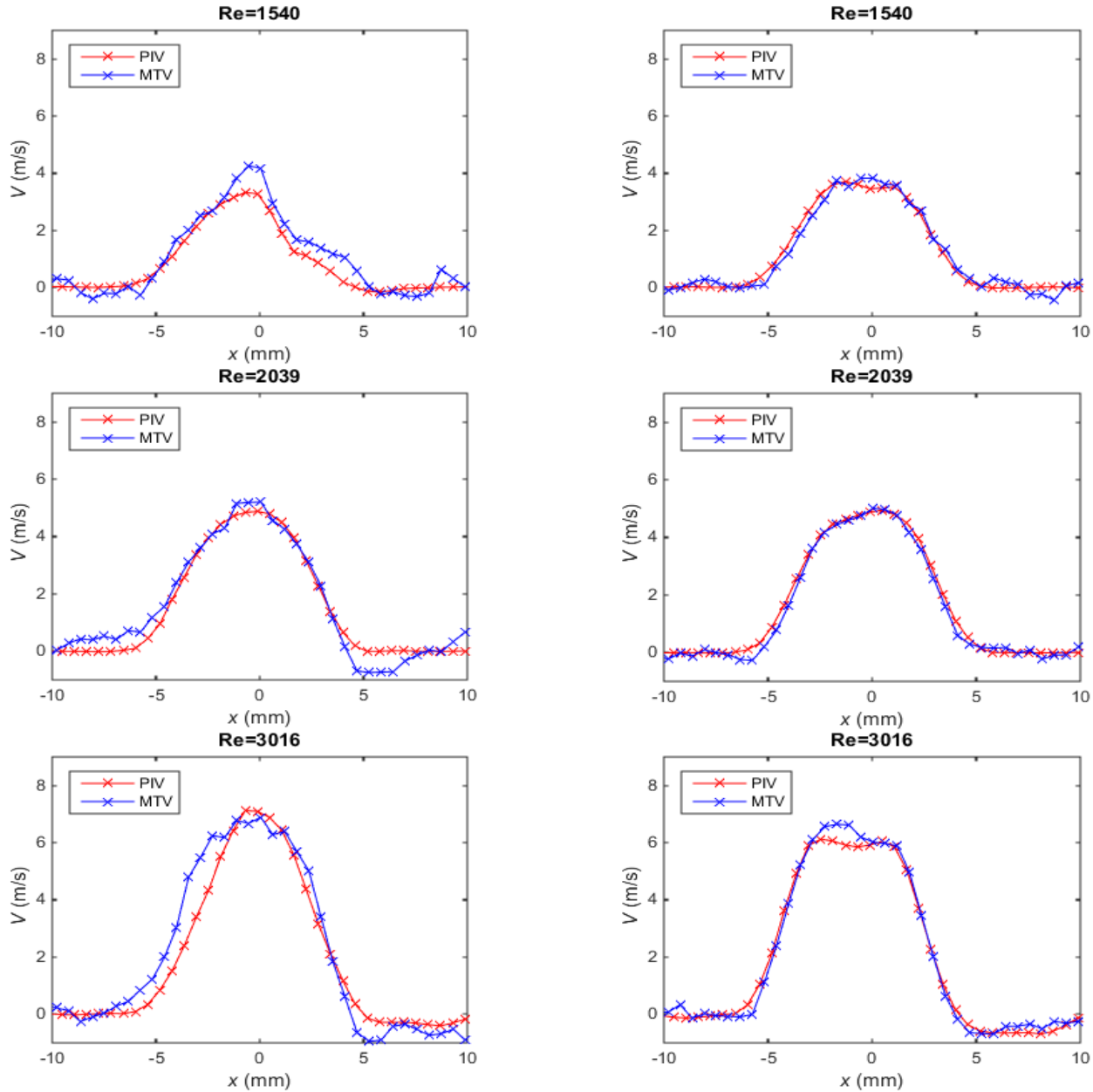


Fig. 7 Instantaneous velocity profiles from HTV (blue) and PIV (red) for the three flow regimes. Typical case (RMS error equal to the median) is shown on the left, and best case (minimum RMS error) is shown on the right.

d. PIV/HTV mean profiles comparison

Mean profiles for the three cases presented in table 1 are plotted in Fig. 8. The RMS error is equal to 2.7%, 2.3%, and 4.7% for $Re=1,540$, $Re=2,039$, and $Re=3,016$. The asymmetry in the profile at $Re=2,039$ is well captured by both techniques. The measured RMS velocity, which correlates strongly with the measurement precision, is lower (better) for PIV than for HTV. Outside the jet, the observed RMS fluctuations were nearly zero in the PIV data, but were, in contrast, up to 0.3 m/s in the HTV data. Note that in more favorable experimental conditions (higher temperature), precision down to 0.1 m/s was obtained on averaged profiles with this technique using the same experimental apparatus [André, 2016]. For $Re=3,016$, the presence of turbulence increases the RMS velocity fluctuations, particularly in the shear layers of the jet; this feature is captured by both methods.

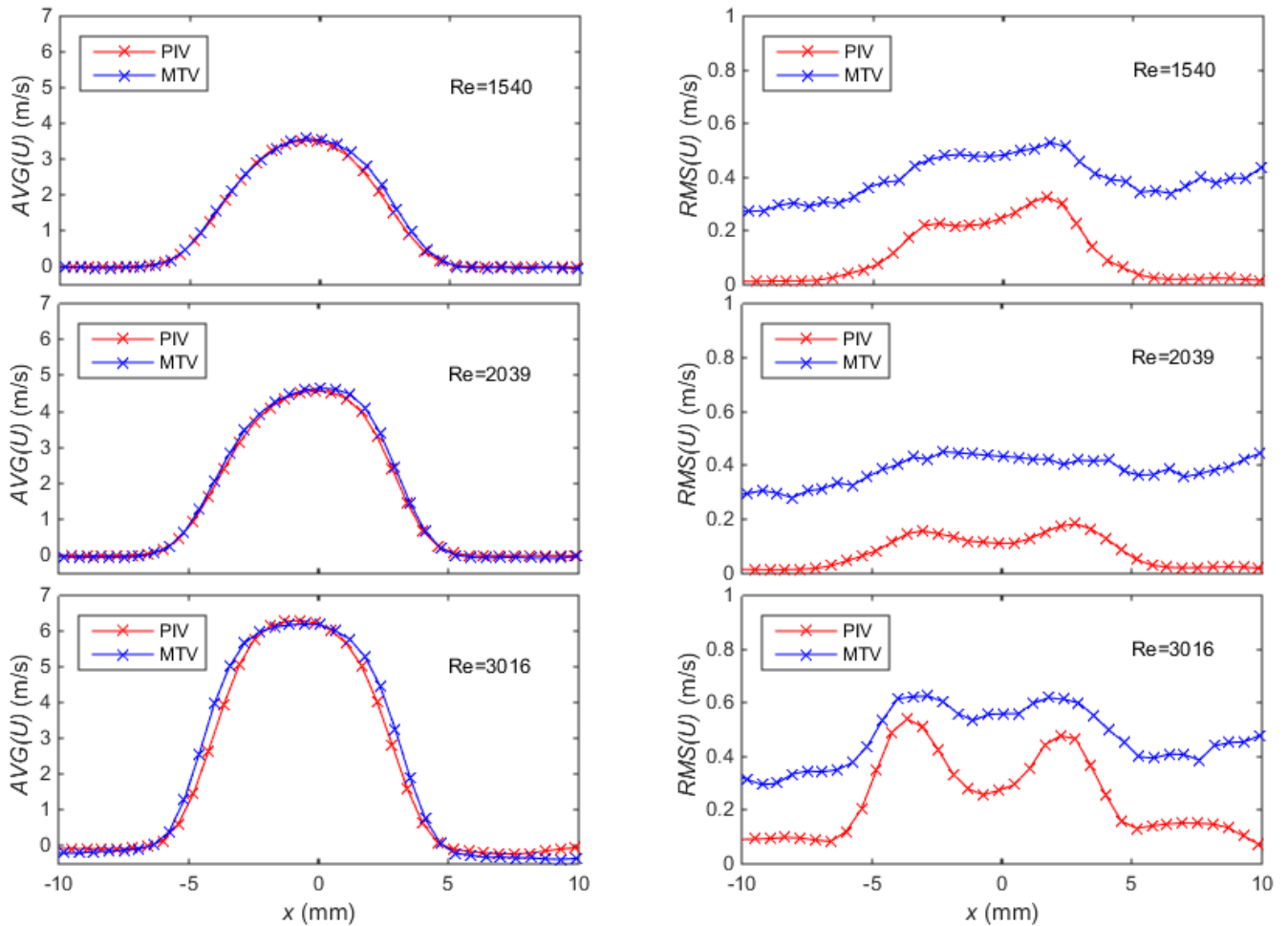


Fig. 8 Comparison of mean (left) and RMS (right) of velocity profiles from PIV and HTV at several Re . Because of the more substantial velocity fluctuations in these regions, a larger error is present in the mean velocity profiles than at the lower Re conditions. Furthermore, the horizontal binning of

the HTV data as well as the relatively large size of the PIV interrogation windows make it difficult to accurately resolve this region of large horizontal velocity gradient.

4. Conclusions

Velocity profiles in a heated N₂ jet were measured with PIV and HTV to assess the performance of HTV in low-speed flow conditions in comparison to an accepted technique. Simultaneous data were recorded by using a single illumination source and splitting the scattered light and fluorescence for independent imaging of the respective signals. Instantaneous and mean profiles for laminar and turbulent jet ($Re = 1540, 2039$, and 3016) were found to compare favorably. Median RMS errors between 9 and 14 percent were observed in the instantaneously velocity profiles, while those of the mean profiles were 2.7, 2.3, and 4.7 percent for the lowest through highest Re conditions. The laminar case provides an estimation of the precision and shows that PIV is more precise than HTV for the conditions examined in this study. The PIV data quality was found to vary inversely with that of the HTV. In order to obtain a better signal in both cases, solid particles such as TiO₂, which survive at higher temperatures, could be used. Furthermore, because of the large difference in signal intensities in the HTV and PIV, the use of a dichroic or more restrictive broadband beam-splitter (80/20 or 90/10 with the bulk of the light going to the HTV) would also improve the magnitudes of the observed signals for both the HTV and PIV.

Acknowledgements

This project was supported by a DOE NEUP grant to Dr. Bardet.

References

- Adrian RJ (2005) Twenty years of particle image velocimetry. *Experiments in fluids*, 39(2), 159-169
- André MA et al. (2015) Development of Hydroxyl Tagging Velocimetry for Low Velocity Flows. *Proceedings of the 2016 AIAA Aviation Conference*, Washington, DC
- André MA et al. (2011) Molecular Tagging Velocimetry development for in-situ measurement in High-Temperature Test Facility. *Proceedings of the 2015 ANS winter meeting*, Washington, DC

- Danehy PM et al. (2003) Flow-tagging velocimetry for hypersonic flows using fluorescence of nitric oxide. *AIAA Journal* 41.2: 263-271
- Luque J and Crosley DR (1999) LIFBASE: Database and Spectral Simulation Program (Version 1.5), SRI International Report MP 99-009
- Pitz RW et al. (2000) Unseeded molecular flow tagging in cold and hot flows using ozone and hydroxyl tagging velocimetry. *Meas. Sci. Tech.* 11.9: 1259
- Ribarov LA et al. (2002) Hydroxyl tagging velocimetry (HTV) in experimental air flows. *App. Phys. B* 74.2: 175-183
- Ribarov LA et al. (2004) Multiline hydroxyl tagging velocimetry measurements in reacting and nonreacting experimental flows. *Exp. Fluids* 37.1: 65-74
- Tropea C, Yarin AL, Foss JF (2007) Springer handbook of experimental fluid mechanics. Springer Science & Business Media